CONSTRUCTION AND TEST OF A CRYOCATCHER PROTOTYPE FOR SIS100*

L. Bozyk, D.H.H. Hoffmann, TU-Darmstadt, Germany and GSI, Darmstadt, Germany
P. Spiller, H. Kollmus, M.Wengenroth, GSI, Darmstadt, Germany

Abstract

The main accelerator SIS100 of the FAIR-complex will provide heavy ion beams of highest intensities. Beam loss due to ionization is the most demanding loss mechanism at operation with high intensity, intermediate charge state heavy ions. A special synchrotron design has been developed for SIS100, aiming for hundred percent control of ionization beam loss by means of a dedicated cryogenic ion catcher system. To suppress dynamic vacuum effects, the cryocatcher system shall provide a significantly reduced effective desorption yield. The construction and test of a prototype cryocatcher is a task of the EU-FP-7 workpackage COLMAT. A prototype test setup, including cryostat has been constructed, manufactured and tested under realistic conditions with beams from the heavy ion synchrotron SIS18. The design and results are presented.

ION CATCHER SYSTEM IN SIS100

The ion optical lattice of SIS100 has been optimized with respect to the implementation of a dedicated ion catcher system [1]. Stripped beam ions are lost at well defined highly localized positions in the cryogenic arcs. Such a peaked loss distribution allows the installation of an efficient ion catcher system with perpendicular low desorption surfaces. Thereby, the amount of charge exchange processes in collisions with residual gas molecules and consecutive ionization beam loss is stabilized during operation.

The basic design considerations of the ion catcher system have been presented in [2]. In the meantime, the prototype has been manufactured, taken into operation, and tested with heavy ion beams from SIS18.

DESIGN OF THE PROTOTYPE CRYOCATCHER AND ITS TEST SETUP

A 3D-model of the cryocatcher and its vacuum chamber is shown in Figure 1. The chamber surrounding the actual cryocatcher acts as a cryopump with high pumping speed. In order to assure a uniform cold temperature distribution, the chamber made of stainless steel is coated with copper. The coating has been explosively plated onto the stainless steel before the chamber was manufactured. Several tests have been performed to guarantee the cryo-suitability of this coating technique. The chamber is connected to a helium supply line via flexible copper straps.

07 Accelerator Technology
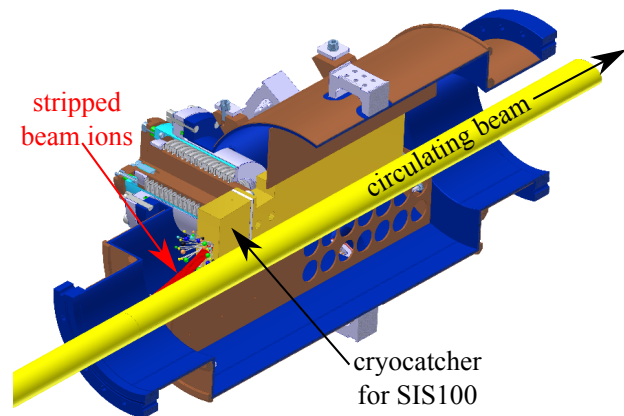
T14 Vacuum Technology

Figure 1: 3D-modell of the cryocatcher prototype with surrounding UHV-chamber (blue) made of stainless steel with an explosively plated copper surface (brown).

The cryocatcher will be kept at a higher temperature than the chamber to avoid freezing-out of gas molecules on the surface of beam impact. To minimize the heat load onto the cooling system, the cryocatcher support acts as a cold-warm-transition. It contains a bellow which provides a high thermal resistance and a separation of the beam vacuum from the insulation vacuum. Because of the limited space in the SIS100 quadrupole cryostat, the mounting with its cold warm transition sticks into the chamber.

The actual support of the cryocatcher consists of a copper block inside the bellow. The block provides a good thermal contact to the warmer side of the bellow. In this way, a thermal contact to the ion catcher from the insulation vacuum is established. The thermal contact is used for connecting the cryocatcher to the thermal shield. Thus the deposited energy of lost ions is dissipated via the shield cooling instead of the chamber cooling.

The cryocatcher itself is a 25 cm long copper block. The length was optimized by FLUKA-simulations [2, 3, 4]. The front part is electrically insulated from the rear part, such that the electrical current of ions hitting the cryocatcher can be measured. The copper catcher has a Nickel-Gold coating, which provides low desorption yields at room temperature [5]. Two different geometries are tested: A block catcher, as indicated in Figure 1, similar to the established catchers in SIS18, and a stair-like catcher, which provides perpendicular incidence and a shielding of the desorbed molecules from the circulating beam.

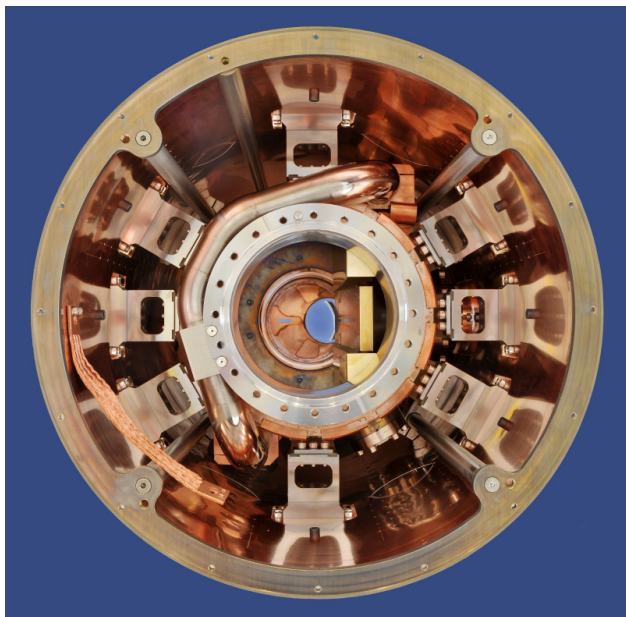The cryocatcher is surrounded by a shielding. This

Figure 2: Picture of the assembled cryocatcher prototype from the backside: The actual cryocatcher (gold) is surrounded by the explosively plated UHV-chamber, which is aligned inside the thermal shield of the test-cryostat.
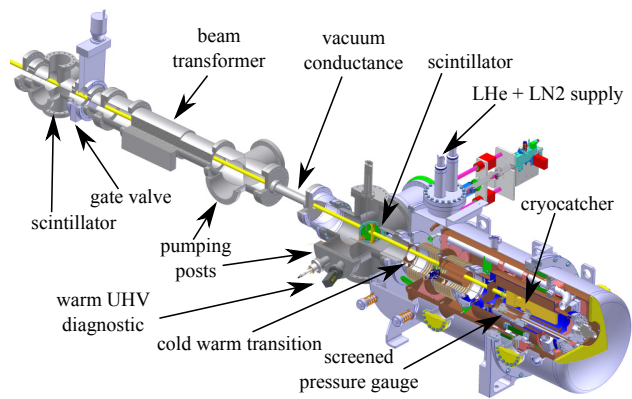

Figure 3: 3D-scetch of the prototype cryocatcher test setup.

shielding prevents the desorbed gases from reaching the beam axis and provides additional cold surfaces for pumping. The position of the cryocatcher inside this secondary chamber minimizes the pressure rise on the beam axis.

The cryocatcher chamber is cooled via flexible copper straps which are connected to a LHe pipe. Both are surrounded by a LN2 cooled thermal shield inside the cryostat chamber. A cold-warm-transition connects the cryocatcher chamber to a warm beam line of the GSI accelerator complex. Different than in SIS100, the prototype is irradiated directly by the primary beam from SIS18.

Figure 2 shows a photography of the assembled prototype cryocatcher inside the thermal shield.

DIAGNOSTICS OF THE PROTOTYPE TEST SETUP

A 3D-modell of the test-setup is shown in Figure 3. During the tests the pressure rise induced by heavy ion bombardment has been investigated. The pressure was measured by a cold penning gauge which is mounted on the backside of the chamber and a thermally shielded hot extractor gauge, which is mounted on a long pipe sticking into the chamber. This pressure gauge allows pressure measurements close to the cryocatcher head surface. In front of the cold-warm-transition, in a warm beam pipe, a further extractor gauge and a residual gas analyzer are situated.

A beam screen situated in the same chamber is used to adjust the beam position. For further control of the beam position during the tests, several plates around the cryocatcher have been mounted electrically insulated. The cur-

rents onto these plates have to be minimized, whereas the current on the cryocatcher has to be maximal.

Since a residual gas pressure of $p < 10^{-11}$ mbar has to be reached inside the cold chamber, a differential pumping system with a small vacuum conductance is installed in front of the setup. Upstream the pumping line a further beam screen is located to assure a parallel incoming beam.

To control the cooling, verify temperature models, and to get reference temperatures for pressure measurements, temperature sensors were mounted onto different components like the LHe-pipe, cold chamber, vacuum gauges, the croycatcher, and its mounting.

TESTING OF THE PROTOTYPE CRYOCATCHER

During the experiments several parameters were investigated, e.g. cooling power, end-pressure, and heavy ion bombardment induced pressure rise as a function of the beam energy and cryocatcher temperature. On the inner chamber temperatures down to 10 K were reached. A transition temperature of ∼18 K, underneath a serious pumping speed for hydrogen emerges, could be verified several times. Each time a lower temperature has been reached, the pressure dropped by two orders of magnitude down to 10^{-12} mbar within several minutes.

The cryocatcher and its mounting showed a quite homogeneous temperature. Fast beam-induced temperature changes on the cryocatcher-head were distributed quickly. The temperature of the support, measured from the insulation-vacuum side, differs only slightly from the cryocatcher's head, i.e. the deposited energy can be dissipated.

During three beam tests the ion beam induced pressure rise was investigated. The two different catcher geometries were tested with Gold and Tantalum beams at energies between 50 MeV and 800 MeV. During the Ta-beamtime, a test at room temperature has been performed. The stair-like catcher was tested with Bismuth ions at beam energies between 100 MeV and 600 MeV. Each time fast extraction was used, with intensities of up to $2 \cdot 10^9$ ions/spill.

07 Accelerator Technology
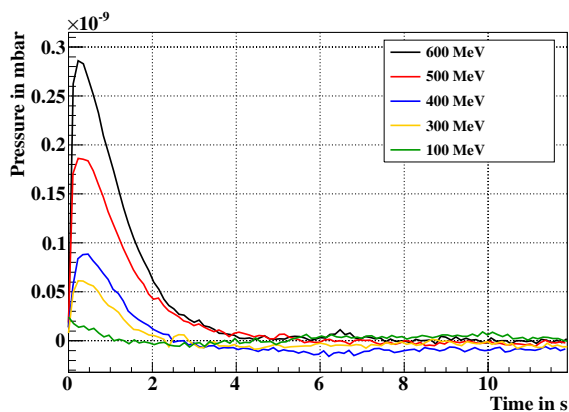
T14 Vacuum Technology

Figure 4: Some exemplarily pressure developments after beam impact onto the cryocatcher for different Bi-beams.

For selected energies, the cryocatcher's temperature was varied between 35 K and 90 K.

The ion current of the extractor gauge situated next to the cryocatcher head was measured with an external ampere meter. Thereby, a fast pressure measurement, triggered by the incoming beam, could be realized. Figure 4 shows some exemplarily pressure developments for different impact energies.

The base pressure after relaxation and the peak pressure were determined for each measurement. The difference, normalized to the number of incident particles, determines the effective pressure rise.

RESULTS

All pressure measurements were corrected by the temperature of the vacuum gauge. After cooling the chamber below 18 K, a base pressure in the lower 10^{-12} mbar regime was reached. The normalized effective pressure rise was measured for different beam energies and temperatures of the cryocatcher. From room-temperature experiments, a dE/dx-scaling of the pressure rise, i.e. a decrease with rising energy is known [6, 7]. During the cold tests, a contrary behavior could be observed: The pressure rise increases with rising energy, see Figure 5. Using the same setup but at room temperature, the pressure rise drops with increasing energy, as expected.

In the investigated temperature range no real dependence of the effective pressure rise from the cryocatcher's temperature could be observed (see Figure 6). Although vapor pressure curves were crossed during the cooldown processes, no pressure drop could be observed in this temperature interval. This means only cryoadsorption and no cryocondensation plays a role.

Comparing the results carefully, the stair-like cryocatcher data in Figure 5 seem to rise slightly less than the block data, although Bismuth is heavier than Gold and Tantalum. Beam impacts were seen in the slow pressure measurement of the cold cathode ion gauge only using the
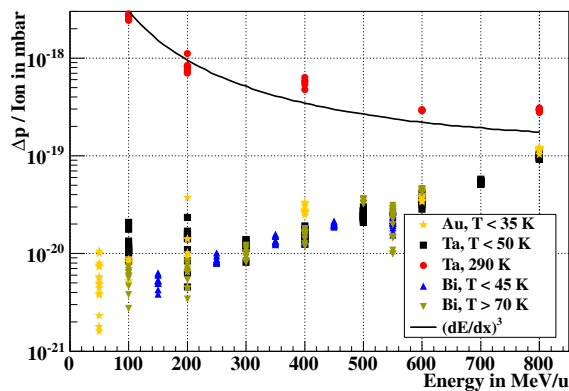
Figure 5: Effective pressure rises as a function of the beam energy for all measurements and different cryocatcher temperatures.
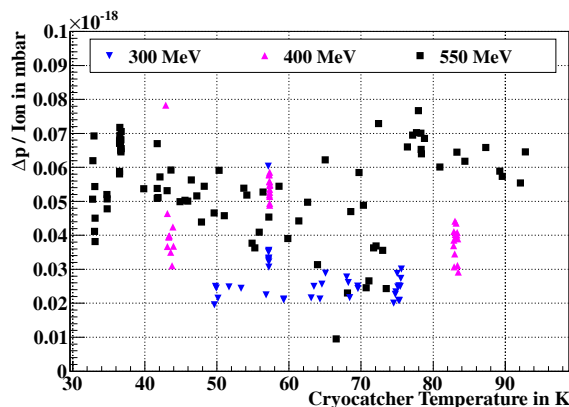

Figure 6: Effective pressure rise as a function of the cryocatcher's temperature for different Bi-beam energies.

block cryocatcher. This indicates that the pressure rise using the stair-like cryocatcher is less pronounced.

The StrahlSim code was used to verify the stability of the dynamic vacuum in SIS100 [8]. Considering the described energy scaling of the desorption yields, the results show a stable operation of SIS100 even at highest heavy ion beam intensities.

REFERENCES

[1] P. Spiller et al., Proc. of ICFA04 (2005)

[2] L. Bozyk et al., Proceedings of IPAC'10 (2010)

[3] G. Battistoni, et al., Proc. of Hadronic Shower Simulation Workshop 2006

[4] A. Fasso et al., CERN-2005-10 (2005), INFN/TC_05/11, SLAC-R-773

[5] M. Bender, Dissertation, Goethe-Uni Frankfurt (2008)

[6] H. Kollmus et al., J. Vac. Sci. Technol. A 27, 245 (2009)

[7] A. W. Molvik et al., Phys. Rev. Lett. 98, 064801 (2007)

[8] P. Puppel et al., Proceedings of IPAC'11 (2011).